Electrical isolation of n -type and p -type InP layers by proton bombardment

H. Boudinov, H. H. Tan, and C. Jagadish

Citation: Journal of Applied Physics **89**, 5343 (2001); doi: 10.1063/1.1365063
View online: http://dx.doi.org/10.1063/1.1365063
View Table of Contents: http://scitation.aip.org/content/aip/journal/jap/89/10?ver=pdfcov
Published by the AIP Publishing

Electrical isolation of *n*-type and *p*-type InP layers by proton bombardment

H. Boudinov,[a] H. H. Tan, and C. Jagadish
Department of Electronic Materials Engineering, Research School of Physical Sciences and Engineering, The Australian National University, Canberra, ACT 0200, Australia

(Received 25 October 2000; accepted for publication 19 February 2001)

The evolution of the sheet resistance (R_s) of *n*-type and *p*-type conductive InP layers during proton irradiation and the stability of the formed isolation during postirradiation annealing were investigated. It was found that the threshold dose (D_{th}) to convert the conductive layer to a highly resistive one is different for *n*- and *p*-type samples with similar initial free carrier concentrations. From our results, one infers that the antisite defects and/or related defect complexes formed by the replacement collisions are the carrier trapping centers, where In_P is responsible for electron trapping and P_{In} for the hole trapping. A time dependence of the R_s was observed after each irradiation step to doses of $\cong D_{th}$ and higher. This time variation is related to metastable processes involving free carriers. The thermal stability of the isolation of *n*-type samples is limited to temperatures lower than 200 °C, irrespectively of the irradiated dose. For *p*-type samples the thermal stability of electrical isolation is extended to 450–500 °C. © *2001 American Institute of Physics.*
[DOI: 10.1063/1.1365063]

I. INTRODUCTION

InP offers remarkable applications as a substrate in optical fiber communication systems, high frequency and high-power device applications, due to its outstanding electrical properties such as high electron mobility and high breakdown field. Semi-insulating (SI) InP layers are needed for current confinement in buried heterostructure lasers,[1] Schottky barrier enhancement and dark current reduction in metal–semiconductor–metal photodetectors,[2] and for inter-device isolation in integrated circuits.[3] Fe is still the commonly used dopant to fabricate SI InP. Ion implantation doping plays a fundamental role in the development of discrete devices and integrated circuits in III–V compound semiconductor technology. Besides this widely used application, the implantation of light mass ions has been proven as a successful method to achieve high resistivity layers in III–V semiconductor devices. An implant isolated region in a semiconductor device may be used as a potential alternative to mesa etching, offering simplicity, precise depth control, and compatibility with planar technology.[4,5] The ion implantation technique for electrical isolation will hereafter be called ion irradiation. The degree of electrical isolation after ion irradiation and low temperature annealing (100–500 °C) is sometimes superior to that provided by mesa structures. Ion irradiation with light ions is very attractive, due to the large penetration depth (>1 μm) for low and medium implantation energies (<1 MeV). In the case of GaAs, high resistivity regions ($>10^7$ Ω cm) can be produced by radiation damage of *n*- or *p*-type material using implantations of ions such as H^+, He^+, B^+, or O^+.[6] The isolation results from the trapping of free carriers by deep level centers that are not thermally ionized at the normal device operating temperature.[4] These deep levels formed by ion irradiation were found to be antisite-related defects.[6] Implantation damage has been utilized in *n*- and *p*-type InP for the reduction of the free carrier concentration.[7–11] However, in contrast to GaAs where excellent electrical isolation has been obtained by ion bombardment, ion irradiation in InP is not as effective in creating high resistivity regions. It has been reported[7,8,12] that the resistivity of *n*-type material can only be increased by ion bombardment to the 10^3 to 10^4 Ω cm range. Although it is possible to make *p*-type InP more resistive[7,13,14] (10^7 Ω cm), the implant dose is critical. Above the optimum dose range the bombarded region becomes slightly *n*-type because of the damage-induced defects which act as donors and the resistivity drops to the 10^3 to 10^4 Ω cm range again.[7] Although implantation isolation is currently used in III–V integrated circuits and discrete device technologies[15,16] a systematic study of the dependence of the threshold dose for isolation and thermal stability with the ion dose is still lacking and the physical processes involved are not yet completely understood. In this work the evolution of the sheet resistance (R_s) and the thermal stability of the electrical isolation of *n*-type and *p*-type InP layers bombarded with protons was studied as a function of the irradiation dose. Antisite defect concentration was taken into account to discuss the results.

II. EXPERIMENT

SI liquid encapsulated Czochralski InP wafers of (100) orientation, with Fe doping in the range of 10^{16} to 10^{17} cm^{-3} were used in this work. After cleaning, the wafers were implanted with ^{28}Si at the energy of 120 keV to the dose of 6×10^{12} cm^{-2} (samples ***n***), in order to create a *n*-type layer. Implantations were performed at room temperature (RT) with the substrate tilted 7° off the surface normal direction to minimize channeling effects. The thermal treatment and dopant activation were carried out with capless (InP proximity) rapid thermal annealing (RTA) at 700 °C for 10 s in flowing

[a]Permanent address: Instituto de Física, UFRGS, Porto Alegre, R.S., Brazil; electronic mail: henry@if.ufrgs.br

TABLE I. Sheet resistance (R_s), effective mobility (μ_{eff}), sheet carrier concentration (C_s), effective layer depth (d), and bulk carrier concentration (C) of the InP samples used in this work.

Sample	R_s [Ω/sq]	μ_{eff} [$\text{cm}^2\,\text{V}^{-1}\,\text{s}^{-1}$]	C_s [cm^{-2}]	d [μm]	C [cm^{-3}]
n	650	2410	$n_s=3.9\times10^{12}$	0.33	$n=1.2\times10^{17}$
p	2530	130	$p_s=1.9\times10^{13}$	1	$p=1.9\times10^{17}$

argon. The thickness of the *n*-type doped layers where the Si atom concentration exceeds 10^{16} cm^{-3} is about 320–350 nm, as calculated by TRIM.[17] The *p*-type samples for this work (samples ***p***) were grown on SI InP substrates with the (100) axis 2° off normal orientation using the ANU metal–organic chemical-vaor deposition reactor. The growth temperature was at 630 °C and the reactor pressure at 76 Torr. The samples were 1 μm thick and doped to a carrier concentration of 1.9×10^{17} cm^{-3}, using Zn as the dopant. The corresponding electrical characteristics of both sets of samples are shown in Table I.

Resistors of rectangular geometry (6×3 mm^2) and square (5×5 mm^2) Van der Pauw[18] devices were prepared from cleaved pieces of samples ***n*** and ***p***. The ohmic contacts to the samples ***n*** were fabricated by applying In and sintering at 250 °C for 2 min. The In contacts formed the mask, which prevented isolation of the covered regions by the subsequent proton irradiation. Ohmic contacts for samples ***p*** were formed by thermal evaporation of Au/Zn/Au (20 nm/200 nm/500 nm) and subsequent annealing at 400 °C for 60 s in an argon ambient at atmospheric pressure. Because the thickness of Au/Zn/Au was not sufficient to prevent the isolation of the covered regions by ion irradiation, additional masking of the contacts was done with aluminum foil.

The resistors were irradiated at RT with $^1\text{H}^+$ at 600 keV to doses in the range of 1.0×10^{12}–1.0×10^{16} cm^{-2}, with an ion current density <0.1 $\mu\text{A/cm}^2$. The energy of the proton beam was chosen to place the damage peak beyond the doped layer. In this way the defect concentration in the doped layer is essentially uniform along the depth. To minimize ion channeling the samples were tilted by 7° off the surface normal direction. The sheet resistance (R_s) values during irradiation were measured *in situ* after each dose step without breaking the vacuum in the target chamber. The devices used in the postirradiation annealing study were irradiated to a single dose. The postirradiation annealing cycles were performed in argon atmosphere in a rapid thermal annealing furnace. The samples were heated from RT up to the final temperature with a heating rate of 50 °C/s. After the final temperature was reached it was maintained constant for 60 s. Annealing temperatures from 100 to 600 °C were employed and the annealing cycles were accumulated in the samples. The R_s measurements were performed in the dark using a Keithley 619 electrometer.

III. RESULTS AND DISCUSSION

Figure 1(a) presents the dose and time evolution of R_s during H^+ irradiation at 600 keV of the *n*-type resistor. The curves show three distinct regions. The first region comprises

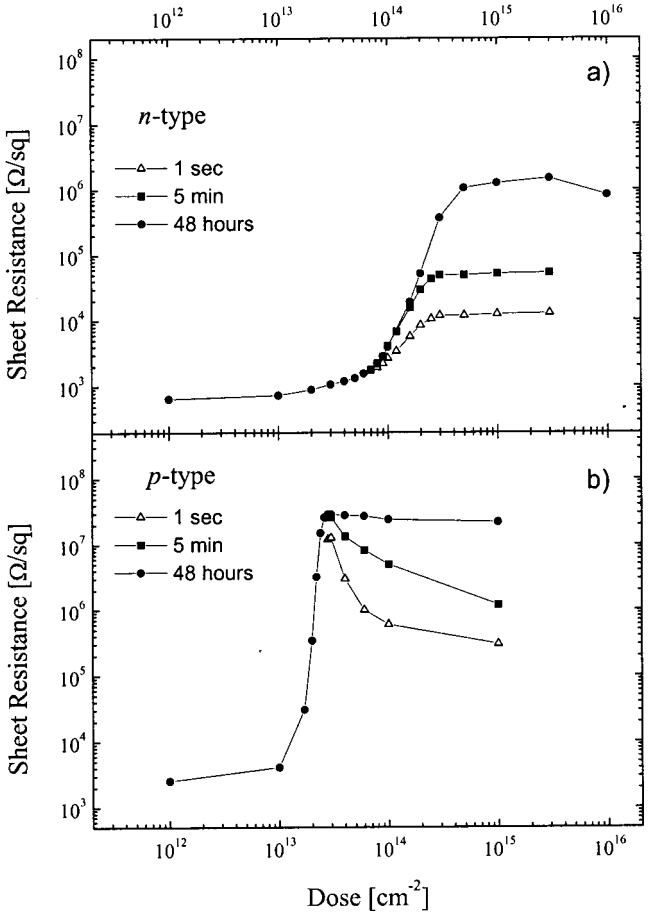

FIG. 1. Time and dose evolution of the sheet resistance of (a) *n*-type ($n=1.2\times10^{17}$ cm^{-3}) and (b) *p*-type ($p=1.9\times10^{17}$ cm^{-3}) InP samples during irradiation with H^+ at 600 keV.

the lowest doses where R_s increases only slightly with the dose. The second region is characterized by a sharp increase of R_s by several orders of magnitude with increasing dose. Carrier trapping at defects created by the irradiation and possibly carrier mobility degradation by the damage cause the change of R_s. The R_s values reach their highest levels after a specific dose has been accumulated (D_{th}, hereafter called threshold doses). The third region is formed by the dose accumulation beyond D_{th}. The values of R_s remain approximately constant, forming a plateau, which extend up to the maximum dose used in this work (4×10^{15} cm^{-2}). In similar experiments of isolation formation in *n*-type or *p*-type GaAs layers[6,19] the value of the measured resistance in the plateau region results from the parallel association of the isolated layer resistance and that of the SI substrate. In the case of InP we have observed a strong time variation of the R_s after finishing the bombardment dose step for total doses of $\cong D_{\text{th}}$ and higher. For this reason it is not correct to relate the R_s value in the plateau with the substrate resistance for times less than 48 h.

The values of R_s for different time intervals after finishing the irradiation dose step have been presented ($t_1=1$ s, $t_2=5$ min, $t_3=48$ h). After 48 h the R_s values reach a saturation and no change was observed in further measurements. Interestingly, the 48 h curve in Fig. 1(a) shows that for very

high doses the plateau region is followed by a decreasing region. This occurs when the damage concentration becomes high enough for the onset of conduction via a hopping mechanism.

Figure 1(b) presents the dose and time evolution of R_s in a *p*-type resistor. The main shape of the curves is similar to that of the *n*-type resistor R_s evolution, but we have to mention some differences. First of all, the threshold doses are $D_{th} \approx 3.0\times10^{14}$ cm^{-2} for the *n*-type and $D_{th} \approx 2.8\times10^{13}$ cm^{-2} for the *p*-type samples. From the data in Table I one can see that the threshold doses for both sets of samples do not scale with the free carrier concentrations. Moreover, the rising slope of the 48 h curve for the *p*-type sample [Fig. 1(b)] is much steeper than the slope of the corresponding curve for the *n*-type sample [Fig. 1(a)]. Consequently, a lower irradiated dose is necessary to isolate *p*-type InP, compared with a *n*-type InP with a similar carrier concentration.

It was demonstrated[20] that for *n*-type InP the ratio between the free electron concentration and the total number of replacement collisions taking place within the doped layer, estimated by TRIM calculations, is a constant after irradiation with D_{th}. Just as in GaAs,[6,19] carrier trapping could be associated with antisite defects (In_P and P_{In}), created in replacement collisions. For the case of *n*-type material the In_P or In_P related acceptor-like defects and for the case of *p*-type material the P_{In} or P_{In} related donor-like defects could play a role of carrier traps.

It has been found[21] that the P_{In} defect has two dominant donor levels: (0/+) and (+/++), with energy levels at 0.11 eV above and 0.23 eV below the minimum of the conduction band, respectively. The relatively low R_s after *n*-type InP complete isolation (10^6 Ω/sq) [see Fig. 1(a)] is very likely due to the autoionization of the P_{In} antisites, via excitation of (0/+) level. The antisite defects in GaAs are responsible for the semi-insulating behavior.[6,22] In InP the presence of these defects seems to have a different character, like traps or self-ionizing donor, depending on the energy level position.[23] Bombarding *p*-type material the holes are trapped in the single charged P_{In} (+/++) antisites or are compensated with the electrons created via autoionization of P_{In} (0/+) antisites. For the *n*-type InP isolation the trapping in In_P antisites competes with the free electron creation via autoionization of P_{In} (0/+) antisites.

As mentioned before, we have observed a strong time variation of the R_s. The time evolution of R_s in *n*-type [Fig. 2(a)] and *p*-type [Fig. 2(b)] samples is shown during the first 5 min after irradiation with different total doses in the range 3.0×10^{13}–3.0×10^{15} cm^{-2}. All curves seem to have an exponential behavior with the time dependence of R_s expressed as

$$R_s(t) = \Sigma a_i[1 - \exp(-t/\tau_i)]. \quad (1)$$

However, it was not possible to fit the data with only one exponential term. By fitting with two exponential terms, a good fit was obtained and the values for the characteristic time constants were $\tau_1 = 5.4 \pm 0.8$ s and $\tau_2 = 80 \pm 11$ s for *n*-type samples and $\tau_1 = 9.6 \pm 1.8$ s and $\tau_2 = 140 \pm 32$ s for *p*-type samples. Additional low dose bombardment and electrical measurements proved that this short time variation is related to metastability of the free carriers and probably due to electron capture–emission phenomena from two different metastable traps. The different characteristic time constants for *n*- and *p*-type samples can be explained by considering the slightly different Fermi energy levels in both cases. Long time metastability (>30 min) is shown in Fig. 3. The sheet resistance of *n*-type resistors, irradiated to different total doses changes linearly with the time up to 48 h after the irradiation. After this time interval the R_s values saturate.

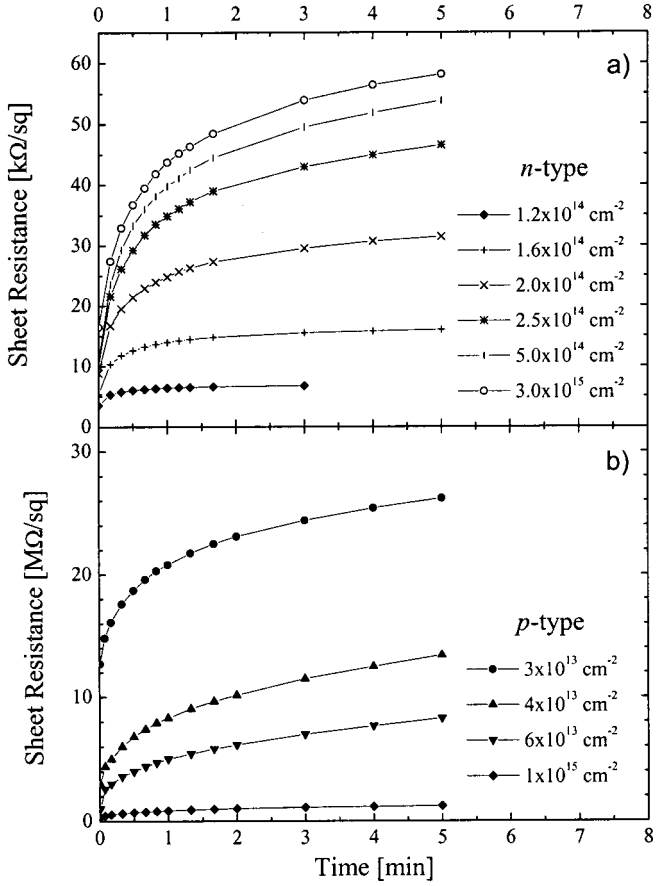

FIG. 2. Time evolution of the sheet resistance of (a) *n*-type and (b) *p*-type InP samples after irradiation with H^+ at 600 keV to different doses.

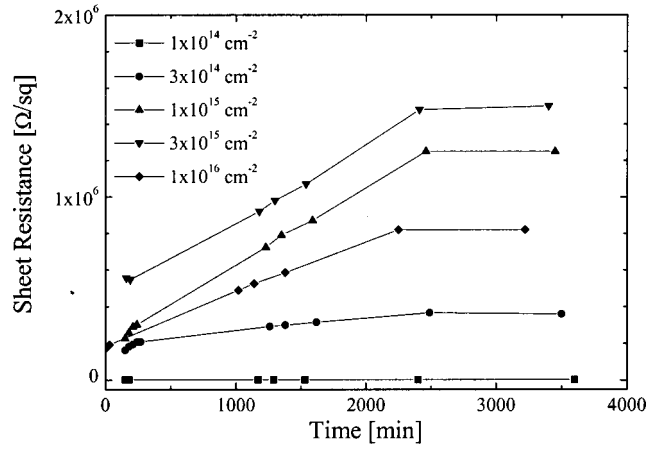

FIG. 3. Long time metastability of the sheet resistance of *n*-type InP samples after irradiation with H^+ at 600 keV to different doses.

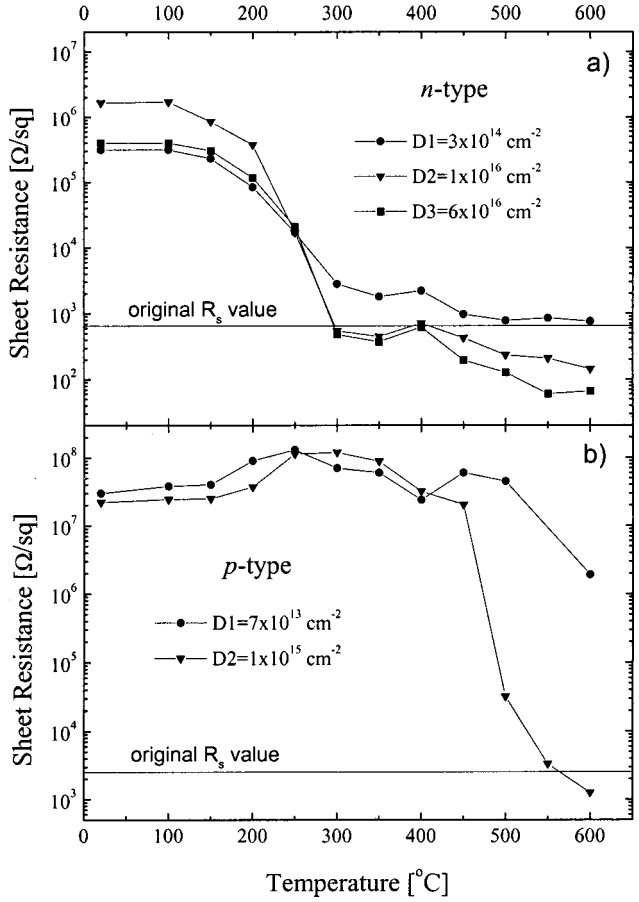

FIG. 4. Evolution of the sheet resistance with temperature after rapid thermal annealing for 60 s in argon atmosphere in (a) *n*-type and (b) *p*-type InP irradiated with H^+ at 600 keV to different doses.

The observed long time sheet resistance metastability is possibly related to room temperature defect annealing, in accordance with previously published results.[24]

The thermal stability of the isolation in *n*-type samples [see Fig. 4(a)] was studied using three different H^+ doses ($D1=3\times10^{14}$ cm^{-2}, $D2=1\times10^{16}$ cm^{-2}, and $D3=6\times10^{16}$ cm^{-2}). These doses correspond to D_{th}, $33D_{th}$, and $200D_{th}$, respectively. It is interesting to note that the evolution of R_s with the annealing temperature is practically the same, irrespective of the introduced defect concentration level. Although the number of replacement collisions for the highest dose is 200 times higher than in the lowest dose case, no improvement in the thermal stability of the isolation resulted. In all the samples the stability of the isolation is restricted to temperatures below 200 °C. Above this temperature, a rapid decrease of R_s by three orders of magnitude is observed. Considering that the In_P antisite defects are double acceptors [like Ga_{As} antisites in GaAs (Ref. 19)] their annealing would produce the observed decreasing of R_s due to releasing of the captured electrons. Probably the In_P antisites defects are annealed at temperatures of 200–300 °C via recombination with In vacancies. We can conclude from the results presented in Fig. 4(a) that only one kind of defect, with the characteristic annealing temperature region mentioned above, is the major cause for the electron trapping. Another less prominent annealing stage starting at 400 °C is apparent in the curves. According to previous results[20] one can note that in the samples irradiated to high doses ($\geqslant 1\times10^{16}$ cm^{-2}) the R_s values after 600 °C annealing results are lower than their original value. It is well-known[25] that in implanted InP layers after annealing at temperatures above 450 °C a kind of donor-like defect exists, which adds free electrons to a donor implant and compensates an acceptor implant. Apparently this process is responsible for the creation of additional free electron concentration in the samples irradiated with doses in excess of D_{th} which were annealed at temperatures $\geqslant$400 °C [see curves for doses D2 and D3 in Fig. 4(a)].

Figure 4(b) presents the thermal stability of the isolation in *p*-type samples after irradiation with two different H^+ doses ($D=7\times10^{13}$ cm^{-2} and $D2=1\times10^{15}$ cm^{-2}). These doses correspond, respectively, to $2.5D_{th}$ and $36D_{th}$. The evolution of R_s with the annealing temperature is different, compared to that of *n*-type irradiated samples. For both *p*-type samples the thermal stability of electrical isolation is extended to 450 °C. Above this temperature, a rapid decrease of R_s by four orders of magnitude is observed for the sample implanted with D2 and the R_s value after 600 °C annealing is lower than its original value. It is important to mention here that the conductivity is changed from *p*-type to *n*-type for this sample. This result can be explained by invoking the formation of the same kind of donor-like defect (eventually P_{In} related defect), which is responsible for the creation of additional free electron concentration. The concentration of this defect is proportional to the irradiated dose and for sufficiently high irradiation doses the defect-related free electron concentration exceeds the hole concentration and inverts the conductivity type. This conclusion is confirmed by the result of thermal stability for the sample irradiated to dose D1 [see Fig. 4(b)]. In this case the concentration of the defects is not enough to invert the conductivity type and its thermal stability is even higher (500 °C). The different defect annealing behavior in *n*-type and *p*-type InP is an indication that the traps for electrons and for holes are distinctly different.

IV. CONCLUSION

The evolution of the sheet resistance and the thermal stability of the electrical isolation of *n*-type and *p*-type InP layers irradiated with protons was studied as a function of the irradiation dose. Lower threshold dose is necessary to isolate *p*-type InP, compared to *n*-type InP with a similar free carrier concentration. Probably, the In_P antisite or In_P related acceptor-like defects trap the electrons, and for the case of *p*-type material the P_{In} or P_{In} related donor-like defects could play the role of hole traps. For the *n*-type InP isolation the trapping in In_P antisites competes with the free electron creation via autoionization of P_{In} (0/+) antisites. A strong time variation of the R_s was observed after finishing the irradiation step for total doses of $\cong D_{th}$ or higher. Characteristic time constants of 5.4 and 80 s for the *n*-type samples and of 9.6 and 140 s for the *p*-type samples were estimated. The variation of R_s with time is most likely related to electron capture–emission phenomena from two different metastable traps. Only one kind of defect, with a characteristic anneal-

ing temperature region of 200–300 °C, is the major cause for the trapping of electrons. Irrespective, of the irradiated dose the thermal stability of implant-isolated *n*-type InP is limited to temperatures lower than 200 °C. The thermal stability of defects responsible for isolation in *p*-type InP is found to be as high as 500 °C. With increasing irradiation dose a decrease of this temperature is observed. High dose implantation and subsequent annealing of *p*-type InP layers leads to *n*-type conversion.

ACKNOWLEDGMENT

This work was partly supported by Conselho Nacional de Pesquisas (CNPq, Brazil) under Contract No. 200541/99-4.

[1] H. Wada, H. Horikawa, Y. Matsui, Y. Ogawa, and Y. Kawai, Appl. Phys. Lett. **55**, 723 (1989).
[2] L. Yang, A. S. Sudbo, R. A. Logan, T. Tanbun-Ek, and W. T. Tsang, IEEE Photonics Technol. Lett. **2**, 56 (1990).
[3] M. Pütz, J. Cryst. Growth **107**, 806 (1991).
[4] S. J. Pearton, Mater. Sci. Rep. **4**, 313 (1990).
[5] S. J. Pearton, Int. J. Mod. Phys. B **7**, 4687 (1993).
[6] J. P. de Souza, I. Danilov, and H. Boudinov, Appl. Phys. Lett. **68**, 535 (1996).
[7] J. P. Donnelly and C. E. Hurwitz, Solid-State Electron. **20**, 727 (1977).
[8] P. E. Thompson, S. C. Binari, and H. B. Dietrich, Solid-State Electron. **26**, 805 (1983).
[9] M. W. Focht, A. T. Macrander, B. Schwartz, and L. C. Feldman, J. Appl. Phys. **55**, 3859 (1984).
[10] S. J. Pearton, C. R. Abernathy, M. B. Panish, R. A. Hamm, and L. M. Lunardi, J. Appl. Phys. **66**, 656 (1989).
[11] V. Sargunas, D. A. Thompson, and J. G. Simmons, Nucl. Instrum. Methods Phys. Res. B **106**, 294 (1995).
[12] M. C. Ridgway, R. G. Elliman, M. E. Faith, P. C. Kemeny, and M. Davies, Nucl. Instrum. Methods Phys. Res. B **96**, 323 (1995).
[13] M. W. Focht and B. Schwartz, Appl. Phys. Lett. **42**, 970 (1983).
[14] M. C. Ridgway, C. Jagadish, R. G. Elliman, and N. Hauser, Appl. Phys. Lett. **60**, 3010 (1992).
[15] F. Clauwaert, P. Van Daele, R. Baets, and P. Lagasse, J. Electrochem. Soc. **134**, 711 (1987).
[16] S. J. Pearton, C. R. Abernathy, J. W. Lee, F. Ren, and C. S. Wu, J. Vac. Sci. Technol. B **13**, 15 (1995).
[17] J. F. Ziegler, J. P. Biersack, and U. Littmark, in *The Stopping and Range of Ions in Solids* (Pergamon, Oxford, 1985), Vol. 1.
[18] L. J. Van der Pauw, Philips Res. Rep. **13**, 1 (1958).
[19] J. P. de Souza, I. Danilov, and H. Boudinov, J. Appl. Phys. **81**, 650 (1997).
[20] H. Boudinov, J. P. de Souza, and C. Jagadish, Nucl. Instrum. Methods Phys. Res. B (to be published).
[21] P. Dreszer, M. W. Chen, K. Seendripu, J. A. Wolk, W. Walukiewicz, B. W. Liang, C. W. Tu, and E. R. Weber, Phys. Rev. B **47**, 4111 (1993).
[22] M. J. Caldas, J. Dabrowski, A. Fazzio, and M. Scheffler, Phys. Rev. Lett. **65**, 2046 (1990).
[23] P. J. Dean, M. S. Skolnick, B. Cockayne, W. R. MacEwan, and G. W. Iseler, J. Cryst. Growth **67**, 486 (1984).
[24] M. Yamaguchi, Y. Itoh, and K. Ando, Appl. Phys. Lett. **45**, 1206 (1984).
[25] B. Molnar, T. A. Kennedy, E. R. Glaser, and H. B. Dietrich, J. Appl. Phys. **74**, 3091 (1993).